ORIGINAL ARTICLE

JBMR®

Age-Related Changes in the Mechanical Regulation of Bone Healing Are Explained by Altered Cellular Mechanoresponse

Edoardo Borgiani,[1,2]* Christine Figge,[1]* Bettina Kruck,[1] Bettina M Willie,[3] Georg N Duda,[1,2]** and Sara Checa[1,2]**

[1]Julius Wolff Institute, Charité - Universitätsmedizin Berlin, Berlin, Germany
[2]Berlin-Brandenburg School for Regenerative Therapies, Berlin, Germany
[3]Research Centre, Shriners Hospital for Children-Canada, Department of Pediatric Surgery, McGill University, Montreal, Canada

ABSTRACT

Increasing age is associated with a reduced bone regeneration potential and increased risk of morbidities and mortality. A reduced bone formation response to mechanical loading has been shown with aging, and it remains unknown if the interplay between aging and mechanical stimuli during regeneration is similar to adaptation. We used a combined in vivo/in silico approach to investigate age-related alterations in the mechanical regulation of bone healing and identified the relative impact of altered cellular function on tissue patterns during the regenerative cascade. To modulate the mechanical environment, femoral osteotomies in adult and elderly mice were stabilized using either a rigid or a semirigid external fixator, and the course of healing was evaluated using histomorphometric and micro-CT analyses at 7, 14, and 21 days post-surgery. Computer models were developed to investigate the influence of the local mechanical environment within the callus on tissue formation patterns. The models aimed to identify the key processes at the cellular level that alter the mechanical regulation of healing with aging. Fifteen age-related biological alterations were investigated on two levels (adult and elderly) with a design of experiments setup. We show a reduced response to changes in fixation stability with age, which could be explained by reduced cellular mechanoresponse, simulated as alteration of the ranges of mechanical stimuli driving mesenchymal stem cell differentiation. Cellular mechanoresponse has been so far widely ignored as a therapeutic target in aged patients. Our data hint to mechanotherapeutics as a potential treatment to enhance bone healing in the elderly. © 2019 American Society for Bone and Mineral Research.

KEY WORDS: BONE HEALING; CELLULAR MECHANORESPONSE; COMPUTER MODELING; AGING

Introduction

Increasing age is associated with a reduced bone regeneration potential,[1,2] longer hospitalization stays,[3] and increased risk of morbidities and mortality.[4] Changes in multiple cellular processes might contribute to the altered bone-healing response with age. Reductions in the number of stem cells,[5] migration,[6] proliferation or differentiation capacity,[7,8] altered revascularization,[9] as well as altered tissue material properties[10,11] have all been associated with a reduced regenerative capacity with increasing age. However, which of these components mainly contribute to the alterations observed at the tissue level remains poorly understood. Identifying key players involved in age-related alterations in regeneration appears essential for the development of an effective therapeutic strategy. Experimentally, it is challenging to determine the contribution of individual biological events at the cellular or tissue levels in relation to the overall bone regeneration process. Computer modeling techniques allow one to integrate data on different biological scales and to investigate the role of processes at the cellular scale and thereby formulate more specific hypotheses on what impacts tissue patterning during the course of healing.[12]

Next to biological signals, mechanical stimuli play a key role in bone regeneration.[13–15] During the last decades, intensive research has been carried out with the aim to understand the mechanical "rules" driving bone regeneration. Here computer-modeling techniques, based on finite element analyses, have played a key role because they allow one to determine the local mechanical conditions within the healing region, which cannot be experimentally determined. By relating the local mechanical stimuli within the callus to the observed tissue formation patterns over the course of

Received in original form October 2, 2018; revised form April 3, 2019; accepted May 18, 2019. Accepted manuscript online May 23, 2019.
Address correspondence to: Sara Checa, PhD, Julius Wolff Institute, Charité - Universitätsmedizin Berlin, Campus Virchow-Klinikum, Institutsgebäude Süd/Südstraße 2, Augustenburger Platz 1, 13353 Berlin, Germany. E-mail: sara.checa@charite.de
*EB and CF contributed equally to this work.
**GND and SC contributed equally to this work.
Additional Supporting Information may be found in the online version of this article.
Journal of Bone and Mineral Research, Vol. 34, No. 10, October 2019, pp 1923–1937.
DOI: 10.1002/jbmr.3801

healing, ranges of mechanical strain beneficial for intramembranous bone formation, osteochondral ossification, and fibrous tissue formation have been identified.[16–18] Over the last years, these theories have been successfully implemented in computer models and validated against histological data[19–21] to understand the mechanical regulation of tissue repair and differentiation in fracture healing.[22,23] The role played by the local mechanical conditions during the healing process has been investigated by simulating the influence of fixation stiffness,[24] gap size,[25] fracture type,[26] and external loading conditions on healing outcome.[27,28]

In vivo studies of bone adaption have shown that aging reduces the bone (re)modeling response to mechanical loading.[29,30] Specifically, the mechanoresponse of bone-forming cells (osteoblasts) appears to be reduced by increasing age. To date, it remains largely unknown how aging influences the mechanical regulation of bone healing. Experimentally, it has been shown that aging affects the biomechanical properties of the fracture callus under different fixation stabilities.[31] However, no influence of fixation stability in aged animals was shown in terms of callus mineralization or microstructure in rats.[32] In contrast, a recent study showed that stiffer mechanical stabilization reduced interfragmentary strains and prevented bone-healing delays in aged mice.[33] It remains unknown how local mechanical signals within the callus region relate to the tissue formation patterns over the course of healing and which age-related alterations at the cellular level contribute to altered bone regeneration in aged mice.

Therefore, the aim of this study was to identify key cellular processes that impact age-related alterations in the mechanical regulation of bone healing. Using a combined in vivo/in silico approach, we aimed to determine how age-related alterations at the cellular level in terms of cell numbers, cellular mechanoresponse, migration, proliferation, or differentiation potential might contribute to observations at the tissue level.

Materials and Methods

Animals and experimental design

Thirty-six female C57Bl/6J mice (Charles River, Lyon, France), aged 44 to 50 weeks, were group-housed at the animal facility in individually ventilated cages, with a 12-hour light/dark cycle and standardized feeding until they reached the age of 78 weeks. Animals were randomly divided into groups for rigid or semirigid fixation and 7, 14, or 21 days of healing ($n = 6$ per group). These groups were compared with previous experiments in adult mice (26 weeks old) that underwent surgery under the same experimental conditions.[34] The surgery and outcome measures in both experimental series were performed using identical protocols, although not the same personnel. Previously published experimental data (7-, 14-, and 21-day micro-CT; 7-, 14-, and 21-day histomorphometry) from a study examining the effect of sclerostin neutralizing antibody treatment on bone healing in adult mice[34] are included in the current article for comparison with new experimental data from elderly mice. All experiments were approved by the local authorities (LAGeSo G0021/11).

Surgical procedure

For controlled analysis of bone healing, all mice underwent a unilateral diaphyseal femoral osteotomy stabilized either by a rigid or a semirigid external fixator (RISystem AG, Davos, Switzerland) as previously described.[34,35] Briefly, mice were anesthetized with a 2% isoflurane oxygen mixture. The left femur was shaved at the lateral side from the knee to the hip. An approximately 1.5-cm-long incision through the skin was made with a scalpel. The fascia lata was dissected and muscles were bluntly pushed aside from the femur. Using the fixator bar as a stencil, four holes were drilled into the femur and the fixator bar was mounted with mini Schanz screws. A 0.5-mm osteotomy was performed between the inner screws using a Gigli wire saw (RISystem AG). The mice woke up under a heating lamp. Postoperative analgesia was provided by administering 25 mg tramadol hydrocholoride (Tramal, Grünenthal GmbH, Aachen, Germany) per mL in the drinking water for 3 days postoperatively.

Histology

Mice were euthanized 7, 14, or 21 days post-osteotomy. Osteotomized and contralateral femurs were carefully dissected and fixed for 48 hours in 4% paraformaldehyde (Electron Microscopy Sciences, Hatfield, PA, USA). The bones were then washed and the fixator was removed. Femora were decalcified for 14 to 21 days in EDTA (Herbeta-Arzneimittel, Berlin, Germany). Bones were dehydrated automatically in a semi-enclosed benchtop tissue processor (Leica TP 1020, Leica Biosystems Nussloch GmbH, Nussloch, Germany) for 1 day by ascending alcohol, xylene, and finally embedded into paraffin (Paraplast plus, McCormick Scientific LLC, St. Louis, MO, USA). Longitudinal sections of 4-µm thickness were made with a rotary microtome (Leica RM 2055, Leica Biosystems Nussloch GmbH). Sections from the middle of the callus were stained with Movat's pentachrome.

Scoring healing outcome: the bridging score

Bridging of the osteotomy gap was evaluated by two independent observers 21 days post-surgery using Movat's pentachrome–stained sections. The score A was given for complete periosteal and/or intracortical bridging of both cortices with remodeling present, showing a continuity of the marrow cavity. The score B was given for complete bridging of the two cortices with a discontinuous marrow cavity due to the presence of endosteal bone. The score C was given for incomplete intracortical/periosteal bony bridging. The score D was given for endosteal bone formation (without intercortical or periosteal bone formation), and the score E was given for pseudoarthrosis.

Histomorphometry

To conduct the histomorphometry analysis, the Movat's pentachrome sections were digitalized using a transmitted light microscope (Axioskop 40, Carl Zeiss AG, Jena, Germany) with a camera (Axiocam MRc 5, Carl Zeiss AG) and commercial software (AxioVision Release 4.8 software, Carl Zeiss AG). A 1-mm region of interest (ROI) was analyzed, which included the 0.5-mm osteotomy gap and 0.25 mm in the proximal and distal directions. The width of this ROI was individually adapted according to the thickness of each callus. The cortical bone was excluded from the ROI. The different tissue types of the callus in the Movat's pentachrome–stained sections were semi-automatically quantified with commercial software (KS 400 3.0, Carl Zeiss AG). Callus tissue composition was characterized by quantitative analysis of bone, cartilage, and connective tissue

formation, with connective tissue including fibrous tissue and marrow elements. Tissue area (mm^2) was measured and tissue fractions (%) were calculated.

Ex vivo micro-computed tomography analysis

Micro-CT analyses were performed at 7, 14, and 21 days post-osteotomy (Scanco vivaCT 40, Scanco Medical, Brüttisellen, Switzerland) at an isotropic voxel size of 10.5 µm (70 kV and 114 µA). The cortical bone was manually excluded and the callus was included. A global threshold of 546.2 mg HA/cm^3 was used to separate mineralized from nonmineralized tissue. The volume of interest included a region of 1 mm height, centered in the middle of the osteotomy gap, including the whole width of the callus. Bone-healing parameters included mineralized callus volume (BV, mm^3), total callus volume (TV, mm^3), and mineralized callus volume fraction (BV/TV).

Finite element models

Finite element (FE) computer models of the experimental mouse osteotomies were created to determine the mechanical strains induced within the healing region immediately after surgery. The models included the femur, the medullary cavity, the external fixator, and the callus region (Fig. 1). Because bone dimensions were similar in adult and elderly mice, one representative finite element model was developed based on the average dimensions of both groups. The femur was idealized as a hollow cylinder of cortical bone filled with marrow tissue. A 0.5-mm opening was transversely created in the middle of the bone to simulate the fracture gap. The fracture opening and its surrounding area were included in a callus domain. The fractured bone model was then stabilized by including the external fixator. The two fixation systems (rigid, semirigid) used in the experimental setup were modeled (Fig. 1).

FE models were built using commercial software (Abaqus v6.12). The callus size was chosen so that further expansion of the callus region did not influence the predicted strains, as it has been previously reported that callus size influences the mechanical environment in fracture-healing FE models.[36] The models were meshed with tetrahedral elements (C3D8), and a convergence study was carried out to determine the mesh size inside the callus domain. The final average characteristic element length size within the callus domain was 0.1 mm.

The callus was assumed to be initially filled with granulation tissue. Material properties of the FE model were assigned as follows[19]: cortical bone: $E = 5000$ MPa, $\nu = 0.3$; marrow tissue: $E = 2$ MPa, $\nu = 0.167$; granulation tissue: $E = 0.2$ MPa, $\nu = 0.167$. Both unilateral external fixators consisted of four titanium nails ($E = 170$ GPa, $\nu = 0.33$) and a fixator bar made of polyether-etherketone (PEEK) ($E = 3800$ MPa, $\nu = 0.38$).

Compression and bending loads were applied as previously reported.[19] Briefly, in the proximal bone end, a compression load of 1.5 N was applied in combination with a bending moment of 2.7 Nmm. Boundary conditions were applied on the other bone end to restrain the movement in all directions.

Computer simulations of bone healing

Iterative computer models were developed to investigate the mechanical regulation of tissue formation over the course of healing and how it is altered with aging. A combined finite element agent–based approach was followed. Although the approach has been previously reported,[19] the simulations presented here for adult and elderly mice have not been published before. Bone-healing progression was modeled by simulating cellular activity (migration, proliferation, differentiation, apoptosis, matrix synthesis, and degradation) over time and its consequences on tissue patterning. Our approach was

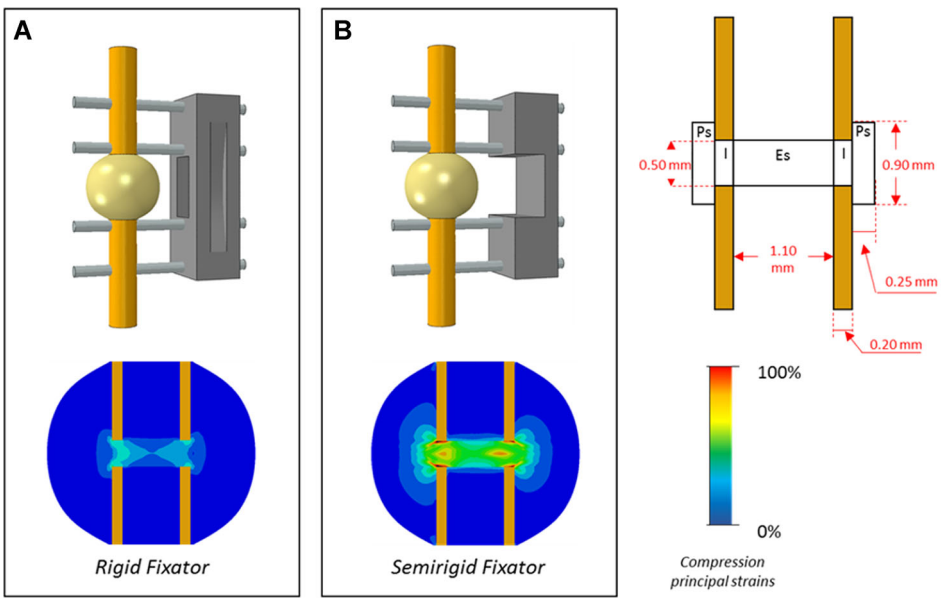

Fig. 1. Finite element models of the mice femoral osteotomy stabilized with a rigid (*A*) and a semirigid fixator (*B*) and predicted compressive principal strain distributions within the callus. Callus regions under investigation and their dimensions are reported. Ps = periosteal; I = intracortical; Es = endosteal.

informed by previous work showing that the differentiation of mesenchymal stem cells (MSCs) into osteoblasts, chondrocytes, or fibroblasts is influenced by the local mechanical stimuli within the healing region.[17] We have previously shown that bone healing in mice takes place under higher mechanical stimuli compared with other species.[19] Therefore, we adapted the ranges of mechanical stimuli leading to osteogenesis, chondrogenesis, and fibrogenesis used in previous investigations on rats[20] to account for the higher mechanical environment encountered within the healing region of mice (Supplemental Materials and Methods). Different cell phenotypes synthesized different types of tissues (bone, cartilage, fibrous tissue) with different mechanical properties that, over time, altered the mechanical conditions within the healing region and, therefore, the progression of healing.

Parametric analysis of the effect of age-related alterations in cellular activity on bone healing

To determine the influence of age-related alterations of cellular activity on bone healing, multiple factors at the cellular level were investigated. A parametric study based on design of experiments was performed to investigate the role of 15 parameters (P1 to P15) on the age-related alteration of bone healing in mice. To each parameter, two levels were associated: adult (+1) and elderly (–1). Previously reported factor values[19] were considered representative of the bone-healing situation in adult mice and used as input parameters of the adult level. To simulate the elderly level, parameter values were either halved (migration, proliferation and differentiation rates, and cell number) or doubled (apoptosis rate) to account for potential age-related effects (Table 1).

Another two parameters were added to investigate the influence of age-related changes in tissue material properties and cellular mechanoresponse. Age-related tissue stiffening (P14) was investigated by increasing 20% the baseline Young's modulus of all the biological materials. Cellular mechanosensitivity (P15) was reduced in the elderly level by moving the ranges of mechanical stimuli driving MSC differentiation into fibroblasts, chondrocytes, and osteoblasts to higher values (Supplemental Materials and Methods).

Table 1. Cellular Activity Parameters Investigated on Two Levels: Adult (+1) and Elderly (–1)

		Levels	
	Parameter	Adult (+1)	Elderly (–1)
Initial MSC density			
Periosteal	P1	30%	15%
Marrow	P2	30%	15%
Migration rate			
MSCs	P3	30 μm/h	15 μm/h
Fibroblasts	P4	30 μm/h	15 μm/h
Differentiation rate			
MSCs	P5	0.3 day^{-1}	0.15 day^{-1}
Proliferation rate			
MSCs	P6	0.6 day^{-1}	0.3 day^{-1}
Fibroblasts	P7	0.55 day^{-1}	0.275 day^{-1}
Chondrocytes	P8	0.2 day^{-1}	0.1 day^{-1}
Osteoblasts	P9	0.3 day^{-1}	0.15 day^{-1}
Apoptosis rate			
MSCs	P10	0.05 day^{-1}	0.1 day^{-1}
Fibroblasts	P11	0.05 day^{-1}	0.1 day^{-1}
Chondrocytes	P12	0.1 day^{-1}	0.2 day^{-1}
Osteoblasts	P13	0.16 day^{-1}	0.32 day^{-1}

MSC = mesenchymal stem cell.

Sixteen different experiments (E1 to E16) were designed to investigate the contribution of each parameter to age-related bone-healing alterations. Orthogonal arrays were used in a Taguchi design of experiments[37] to reduce the number of experiments necessary to investigate interactions between the parameters. Each one of the experiments was characterized by a defined combination of parameters associated with their adult (+1) or elderly level (–1) (Table 2).

The bone tissue area predicted at 7, 14, and 21 days by each of the 16 experiments was used to perform analysis of variance and evaluate the contribution of each parameter to the age-related alteration of bone healing in mice. The sum of the squares of deviation about the mean (SS_F) was calculated for each parameter and, in function of the total sum of squares of the deviation over the mean, the percentage of the total sum of squares (%TSS) was derived. The %TSS represented the contribution of each single parameter to the variance and was considered a measure of the "importance" of each parameter.[12]

The three most influential parameters were then tested for their contribution to age-related alterations in bone healing under both fixation stiffness. All the parameters were assigned to their adult level value except the combination of two or all the three most influential parameters. Bone and cartilage area were predicted for each time point and compared with experimental data from elderly mice.

Statistics

All data were tested for normality using a Shapiro-Wilk test (IBM SPSS Statistics 22, Armonk, NY, USA). ANOVA was used to test the effect of fixator stiffness (rigid versus semirigid), age (adult versus elderly mice), and the interaction between these terms. The statistical analysis of the bridging score was performed using a chi-square test and, in case of a significant difference, with Fisher's exact test. All values are presented as mean ± standard deviation and the level of significance was defined as $p \leq 0.05$.

RESULTS

A greater than twofold increase in mechanical strains was determined within a callus stabilized by a semirigid compared with a rigid fixator

Immediately after osteotomy, average compressive principal strains within the endosteal region were predicted to be 17.9 ± 4.5% in calluses stabilized by rigid fixation. Under semirigid external fixation, average compressive principal strains in the endosteal region were more than two times higher (48.0 ± 15.5%) (Fig. 1). Higher strains were predicted intercortically in the medial side compared with the lateral side (fixator side), both under rigid and semirigid fixation. Also in the intercortical region, average FE-estimated compressive strains were more than two times higher under semirigid than under rigid fixation (rigid fixator intercortical medial side: 26.0 ± 4.7%; rigid fixator intercortical lateral side: 22.5 ± 4.9%; semirigid fixator intercortical medial side: 70.1 ± 14.3%;

Table 2. Orthogonal Matrix With the 16 Experimental Conditions as Combination of the Parameters on Two Levels

	P1	P2	P3	P4	P5	P6	P7	P8	P9	P10	P11	P12	P13	P14	P15
E1	−1	−1	−1	−1	−1	−1	−1	−1	−1	−1	−1	−1	−1	−1	−1
E2	−1	−1	−1	−1	−1	−1	−1	+1	+1	+1	+1	+1	+1	+1	+1
E3	−1	−1	−1	+1	+1	+1	+1	−1	−1	−1	−1	+1	+1	+1	+1
E4	−1	−1	−1	+1	+1	+1	+1	+1	+1	+1	+1	−1	−1	−1	−1
E5	−1	+1	+1	−1	−1	+1	+1	−1	−1	+1	+1	−1	−1	+1	+1
E6	−1	+1	+1	−1	−1	+1	+1	+1	+1	−1	−1	+1	+1	−1	−1
E7	−1	+1	+1	+1	+1	−1	−1	−1	−1	+1	+1	+1	+1	−1	−1
E8	−1	+1	+1	+1	+1	−1	−1	+1	+1	−1	−1	−1	−1	+1	+1
E9	+1	−1	+1	−1	+1	−1	+1	−1	+1	−1	+1	−1	+1	−1	+1
E10	+1	−1	+1	−1	+1	−1	+1	+1	−1	+1	−1	+1	−1	+1	−1
E11	+1	−1	+1	+1	−1	+1	−1	−1	+1	−1	+1	+1	−1	+1	−1
E12	+1	−1	+1	+1	−1	+1	−1	+1	−1	+1	−1	−1	+1	−1	+1
E13	+1	+1	−1	−1	+1	+1	−1	−1	+1	+1	−1	−1	+1	+1	−1
E14	+1	+1	−1	−1	+1	+1	−1	+1	−1	−1	+1	+1	−1	−1	+1
E15	+1	+1	−1	+1	−1	−1	+1	−1	+1	+1	−1	+1	−1	−1	+1
E16	+1	+1	−1	+1	−1	−1	+1	+1	−1	−1	+1	−1	+1	+1	−1

semirigid fixator intracortical lateral side: 61.3 ± 14.1%). Lower mechanical stimuli were predicted in the periosteal region. Compressive principal strains in the periosteal region showed threefold increase under semirigid compared with rigid fixation (rigid fixator periosteal medial side: 13.5 ± 6.0%; rigid fixator periosteal lateral side: 11.5 ± 5.2%; semirigid fixator periosteal medial side: 47.3 ± 16.7%; semirigid fixator medial lateral side: 40.9 ± 16.2%).

In elderly, fixation stiffness did not affect bone-healing progression

In elderly mice, micro-CT analysis did not show significant differences in total callus volume (TV), mineralized callus volume (BV), or mineralized callus volume fraction (BV/TV) between rigid and semirigid conditions at any time point (Table 3). Histological analyses also showed no significant differences in bone or cartilage area between rigid and semirigid conditions in elderly animals at any time point. In elderly mice, only after 21 days of healing, connective tissue was significantly higher in semirigid compared with rigid conditions (Table 3).

Adult and elderly mice have similar healing progression and outcome under rigid fixation conditions

After 21 days of healing, adult and elderly mice stabilized with a rigid fixator showed no significant differences in the callus bridging score (Table 4). In both age groups, most animals showed complete bridging after 21 days (adult: 5/8; elderly: 4/6).

No significant differences in BV/TV could be observed between adult and elderly mice stabilized with a rigid fixator at any time point. Mineralized callus volume (BV) and total callus volume (TV) were not significantly different after 14 and 21 days. Only at day 7, BV was significantly higher in adult compared with elderly mice (Table 3).

Also histologically, bone-healing progression did not appear different in adult and elderly mice under rigid fixation. In both age groups, bone healing occurred through a combination of intramembranous bone formation and endochondral ossification. After 21 days, bone remodeling and bridging of the cortical ends could be observed by histological analyses in both age groups (Fig. 2). No significant differences between adult and elderly mice could be determined in the total bone area or total cartilage area at 7, 14, or 21 days under rigid fixation (Fig. 2). Aging only affected the initial (7-day) callus area; a significantly larger callus formed in adult compared with elderly mice (Fig. 2). Connective tissue area was significantly greater in adult compared with elderly mice under rigid fixation at both 7 days and 21 days post-osteotomy (Fig. 2, Table 3).

Elderly mice had enhanced healing compared with adult mice stabilized with semirigid fixation

After 21 days of semirigid fixation, elderly animals showed significantly better healing scores compared with adult mice ($p = 0.008$) (Table 4). A significantly higher number of elderly mice achieved bony bridging after 21 days compared with adult animals (adult: 1/7; elderly: 5/6).

Histomorphometric analyses showed an increased callus area in adult compared with elderly mice after 7 and 14 days. In addition, connective tissue area was significantly greater in adult compared with elderly mice at 7, 14, and 21 days post-osteotomy. After 21 days, total bone area was significantly higher in elderly compared with adult mice (Table 3). There was no significant difference in cartilage area measured between the adult and elderly mice under semirigid fixation at any of the three time points ($p > 0.08$).

Fracture stabilization plays a more important role in adult than in elderly mice

The influence of fixation stability on bone-healing outcome diminished with aging; semirigid fixation led to a significantly worse healing score than rigid stabilization in adult ($p = 0.005$) but not in elderly mice.

The histomorphometry analysis also showed a stronger effect of fixation stability in adult compared with elderly mice (Fig. 3). In adult mice, total connective tissue area was significantly higher under semirigid compared with rigid conditions at all time points. However, in elderly mice, fixation stability only influenced connective tissue area at day 21.

Micro-CT data also showed an effect of fixation stability in adult but not in elderly mice (Fig. 4). In adult mice, at day 14, total volume (TV), mineralized callus volume (BV), and mineralized callus volume fraction (BV/TV) were significantly

higher under rigid compared with semirigid conditions. In elderly mice, no significant differences were observed in BV, TV, or BV/TV between rigid and semirigid fixation at any time point (Fig. 4).

Age-related alterations in the mechanical regulation of healing can be explained as an alteration of cellular mechanoresponse

Computer model simulations of the bone-healing process were able to predict the overall progression of tissue patterning over the course of healing in adult mice under both rigid and semirigid fixation (Fig. 5). Under rigid fixation, the model predicted initial endosteal bone formation and the formation of cartilage in the osteotomy gap during the first 14 days post-surgery (Fig. 5*A*). Both in vivo (Fig. 3) and in silico, cartilage area increased during the first 2 weeks of healing (Fig. 5*B*). Under semirigid fixation, neither in vivo (Fig. 3) nor in silico, bone bridging was achieved in 2 weeks (Fig. 5*C*). Moreover, under semirigid conditions, both in vivo and in silico, cartilage was still present inside the fracture gap 21 days post-surgery (Fig. 5*D*).

Bone tissue area was predicted for each one of the 16 designed experiments under both rigid and semirigid conditions (Table 5).

Table 4. Callus Bridging Score

	A	B	C	D	E	Total
Adult rigid	2	3	0	0	3	8
Elderly rigid	3	1	0	0	2	6
Adult semirigid	0	0	1	5	1	7
Elderly semirigid	0	4	1	0	1	6

Elderly animals showed a reduced influence of the fixator stability on healing outcome since a higher number of elderly animals showed bony bridging after 21 days in osteotomies stabilized with a semirigid fixator compared with adult animals.

A = periosteal/intracortical bridging between all cortices, remodeling present (continuous marrow cavity).

B = periosteal/intracortical bridging between all cortices, remodeling not present (discontinuous marrow cavity).

C = incomplete bony bridging (periosteal/intracortical).

D = bone formation only endosteal.

E = pseudarthrosis.

Under rigid conditions, in the early stages of healing (7 days), the major role was played by age-related alterations in MSC migration (P3, %TSS = 32%), differentiation (P5, %TSS = 18%), and proliferation (P6, %TSS = 16%) rates. At day 14, reduced cell mechanosensitivity played the main role (P15, %TSS = 36%)

Table 3. Histomorphometry and Micro-CT Analyses at Days 7, 14, and 21 in Adult and Elderly Mice Stabilized With Rigid or Semirigid Fixation

	Adult		Elderly	
	Rigid	Semirigid	Rigid	Semirigid
Day 7	$n = 7$	$n = 9$	$n = 6$	$n = 6$
Total callus area (mm^2)[b]	1.383 ± 0.265[d]	1.571 ± 0.289[d]	0.948 ± 0.130[d]	1.107 ± 0.125[d]
Total bone area (mm^2)	0.041 ± 0.037	0.051 ± 0.075	0.013 ± 0.005	0.02 ± 0.009
Total cartilage area (mm^2)	0 ± 0	0.006 ± 0.007	0 ± 0	0 ± 0
Total connective tissue area (mm^2)[a,b]	1.183 ± 0.227[d,e]	1.508 ± 0.323[d,e]	0.935 ± 0.131[d,e]	1.087 ± 0.126[d,e]
Total volume (mm^3)	1.294 ± 0.173	1.059 ± 0.268	1.051 ± 0.084	1.084 ± 0.146
Mineralized callus volume (mm^3)[b]	0.174 ± 0.036[d]	0.135 ± 0.047	0.111 ± 0.033[d]	0.109 ± 0.025
Mineralized callus volume fraction (mm^3/mm^3)[b]	0.135 ± 0.029	0.126 ± 0.019	0.105 ± 0.027	0.103 ± 0.034
Day 14	$n = 7$	$n = 12$	$n = 6$	$n = 6$
Total callus area (mm^2)[b]	1.483 ± 0.172	2.086 ± 0.519[d]	0.997 ± 0.316	1.282 ± 0.445[d]
Total bone area (mm^2)[a]	0.271 ± 0.150	0.208 ± 0.121	0.288 ± 0.160	0.137 ± 0.140
Total cartilage area (mm^2)[a]	0.054 ± 0.053	0.282 ± 0.318	0.022 ± 0.029	0.178 ± 0.268
Total connective tissue area (mm^2)[a,b,c]	0.850 ± 0.291[e]	1.592 ± 0.295[d,e]	0.687 ± 0.184	0.967 ± 0.255[d]
Total volume (mm^3)[a]	1.702 ± 0.395[e]	1.034 ± 0.257[e]	1.251 ± 0.295	1.040 ± 0.231
Mineralized callus volume (mm^3)[a]	0.525 ± 0.275[e]	0.202 ± 0.063[e]	0.336 ± 0.209	0.111 ± 0.021
Mineralized callus volume fraction (mm^3/mm^3)[a]	0.294 ± 0.112[e]	0.193 ± 0.044[e]	0.256 ± 0.147	0.115 ± 0.049
Day 21	$n = 8$	$n = 7$	$n = 6$	$n = 6$
Total callus area (mm^2)[b]	1.553 ± 0.188	1.877 ± 0.135	0.903 ± 0.188	1.487 ± 0.416
Total bone area (mm^2)[b]	0.245 ± 0.133	0.217 ± 0.114[d]	0.337 ± 0.19	0.458 ± 0.261[d]
Total cartilage area (mm^2)[a]	0.010 ± 0.024	0.214 ± 0.270	0.013 ± 0.022	0.043 ± 0.056
Total connective tissue area (mm^2)[a,b]	0.933 ± 0.394[d,e]	1.394 ± 0.237[d+]	0.553 ± 0.195[d,e]	0.985 ± 0.193[d,e]
Total volume (mm^3)	1.621 ± 0.452	2.395 ± 1.035	1.736 ± 0.602	2.146 ± 0.448
Mineralized callus volume (mm^3)	0.584 ± 0.321	0.548 ± 0.279	0.704 ± 0.324	0.546 ± 0.386
Mineralized callus volume fraction (mm^3/mm^3)[a]	0.336 ± 0.120	0.226 ± 0.0842	0.394 ± 0.137	0.247 ± 0.157

Values reported as mean ± SD. $p < 0.05$ assessed using ANOVA. Adult rigid and adult semirigid data have been previously published[34] and is shown here for comparison.

[a]Effect of fixator.

[b]Effect of age.

[c]Interaction between these terms.

[d]Age effect assessed using *t* test.

[e]Stiffness effect assessed using *t* test.

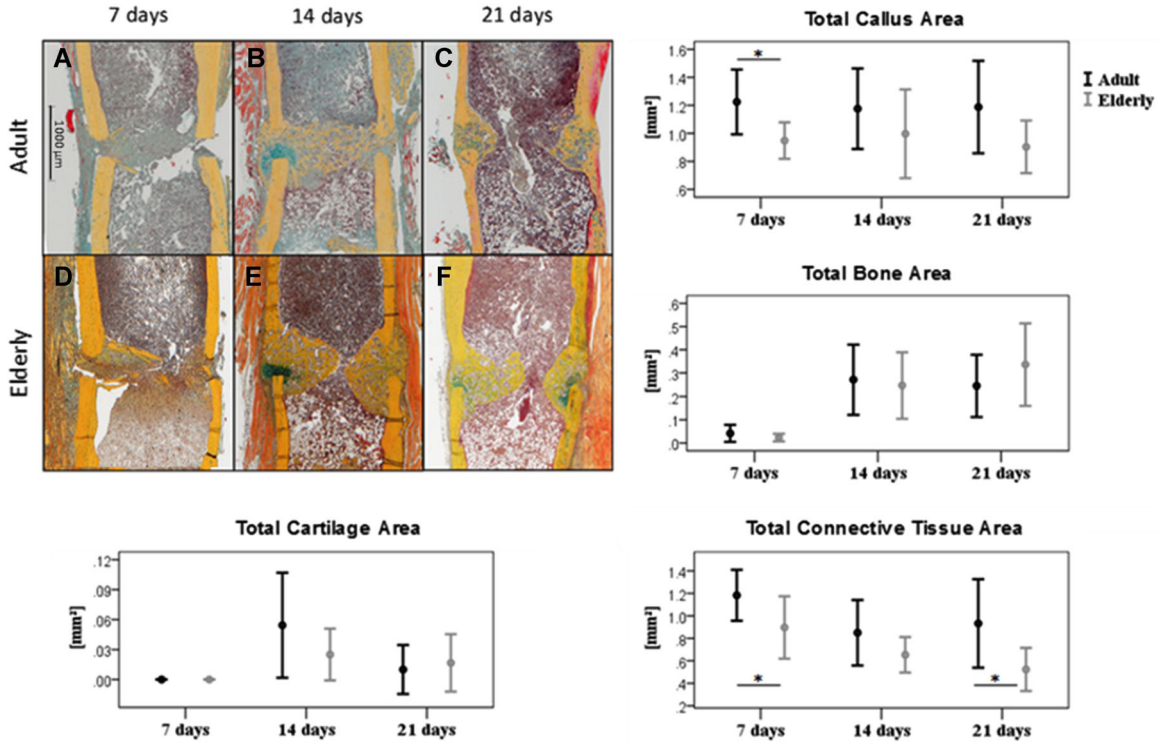

Fig. 2. Representative images of Movat's pentachrome in adult (*A–C*) and elderly (*D–F*) mice after 7 (*A*, *D*), 14 (*B*, *E*), and 21 (*C*, *F*) days with rigid fixation. Histomorphometric quantification of total callus area, total bone area, total cartilage area, and total connective tissue area within the callus at days 7, 14, and 21. Asterisk indicates a significant difference between adult and elderly mice. Note: Histomorphometric data for adult mice were previously published[34] and are provided for comparison to elderly data.

followed by increased fibroblast apoptosis (P11, %TSS = 14%) and decreased MSC migration (P3, %TSS = 12%) rates. At day 21, the most influential aging parameter on bone tissue area was the reduction of cell mechanosensitivity (P15, %TSS = 49%) followed by the increased osteoblast apoptosis ratio (P13, %TSS = 23%) and the reduction of osteoblast proliferation (P9, %TSS = 15%) (Table 6).

Under semirigid conditions, age-related alteration of MSC activities also played a primary role in early stages of healing. At day 7, reduced MSC migration speed (P3, %TSS = 18%) and differentiation rate (P5, %TSS = 11%) were the most influential parameters in addition to increased chondrocyte apoptosis (P12, %TSS = 11%). At day 14, reduced MSC migration speed still played a major role (P3, %TSS = 27%) together with reduced cell mechanosensitivity (P15, %TSS = 27%). The third most influential parameter was the reduced number of MSCs in the marrow cavity (P2, %TSS = 13%). At day 21, three parameters had similar significance in the effect on bone tissue area. Reduced MSC mechanosensitivity (P15), increased fibroblast apoptosis rate (P11), and decreased MSC proliferation ratio (P6) were all characterized by %TSS between 18% and 20% (Table 6). As it was experimentally observed that aging affected more bone healing under semirigid conditions and had almost no effect under rigid fixation, the three parameters that most altered bone healing under semirigid fixation at day 21 were chosen for further analyses.

Predicted tissue distributions under the combination of the most influential aging parameters highlighted the role of reduced mechanosensation (P15). Alterations in tissue patterning under altered mechanosensation were only slightly influenced by two other parameters (P6 and P11) (Figs. 6 and 7). Moreover, under semirigid conditions, only the simulations that included the effect of altered cell mechanosensitivity were able to predict the formation of bone tissue within the fracture gap at days 14 and 21, as observed experimentally in aged mice (Fig. 7).

Quantitative analysis of bone and cartilage area confirmed that age-related alterations of bone healing due to reduced cell mechanosensitivity were only slightly influenced by the other factors (P6 and P11). Whether investigated as single-parameter alteration (P15) or in combination with one (P6 + P15 and P11 + P15) or with both of the other most influential parameters (P6 + P11 + P15), bone and cartilage area followed similar dynamics (Fig. 8).

Comparison of the dynamics predicted by the computer model under age-related alteration of cell mechanosensitivity and bone and cartilage tissue area at 7, 14, and 21 days of the in vivo experiments in elderly mice showed good agreement under rigid conditions.

Under semirigid conditions, the model predicted a steady state in bone formation from day 14. From that time point on, predicted bone tissue area was similar to bone area measured experimentally in elderly mice 21 days post-operation (average 0.46 mm^2). This early response of the model to the healing process was also observed in the cartilage formation dynamics. Histological images from elderly mice under semirigid fixation were characterized by wide cartilage area at 14 days post-operation (average 0.18 mm^2), which tend to reduce due to endochondral ossification at day 21 (average 0.04 mm^2). Analogue dynamics were predicted in advance under aging

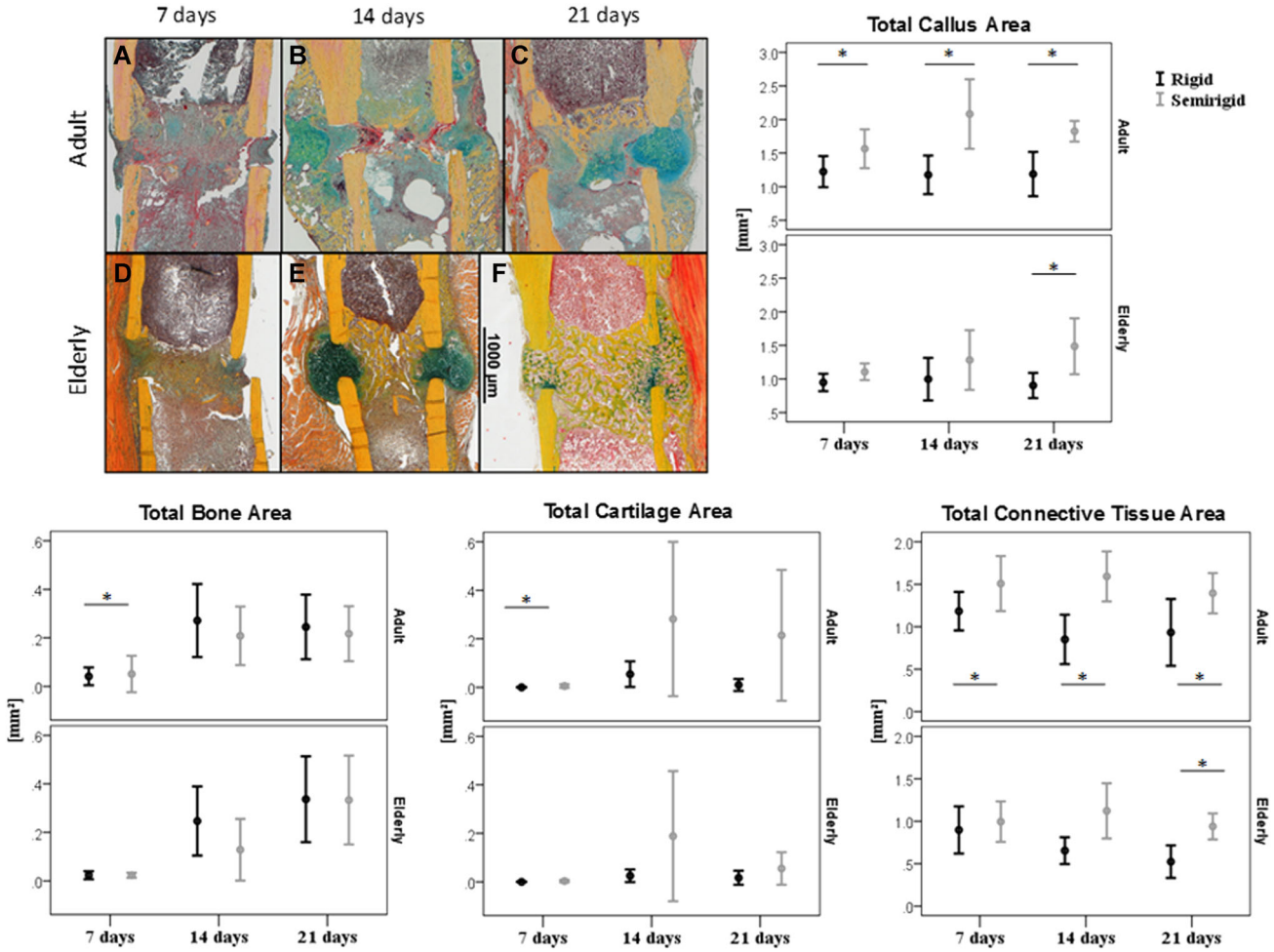

Fig. 3. Representative histological images of healing progression at days 7 (*A*, *D*), 14 (*B*, *E*) and 21 (*C*, *F*) in adult (*A*–*C*) and elderly (*D*–*F*) mice stabilized with a semirigid fixator. Asterisk indicates a significant difference between adult and elderly mice. Note: Histomorphometric data for adult mice were previously published[34] and are provided for comparison to elderly data.

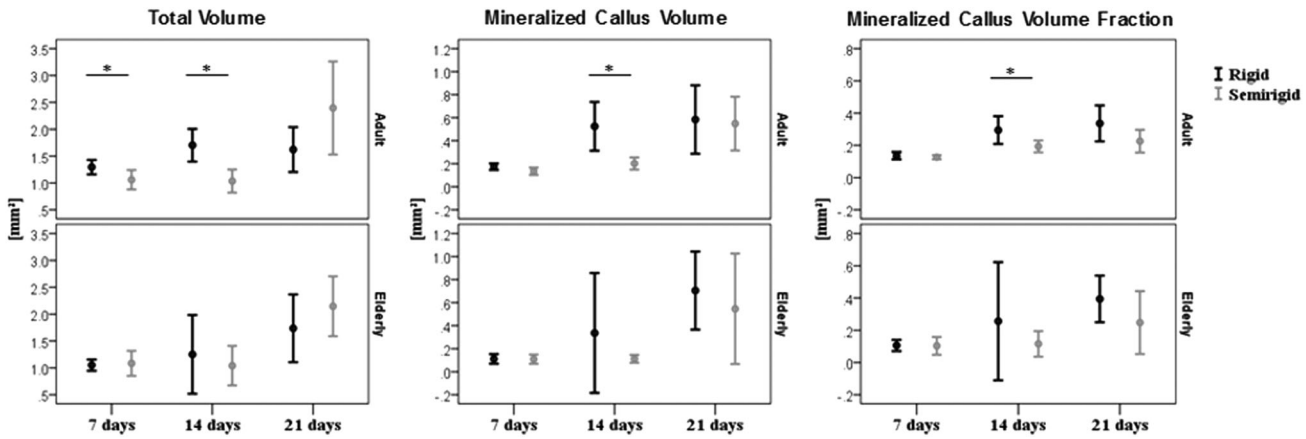

Fig. 4. Influence of fixation stability in micro-CT parameters in adult and elderly mice. Fixation stiffness has a higher influence in adult compared with elderly mice. Asterisk indicates a significant difference between adult and elderly mice within each fixation stiffness. Note: Micro-CT data for adult mice were previously published[34] and are provided for comparison to elderly data.

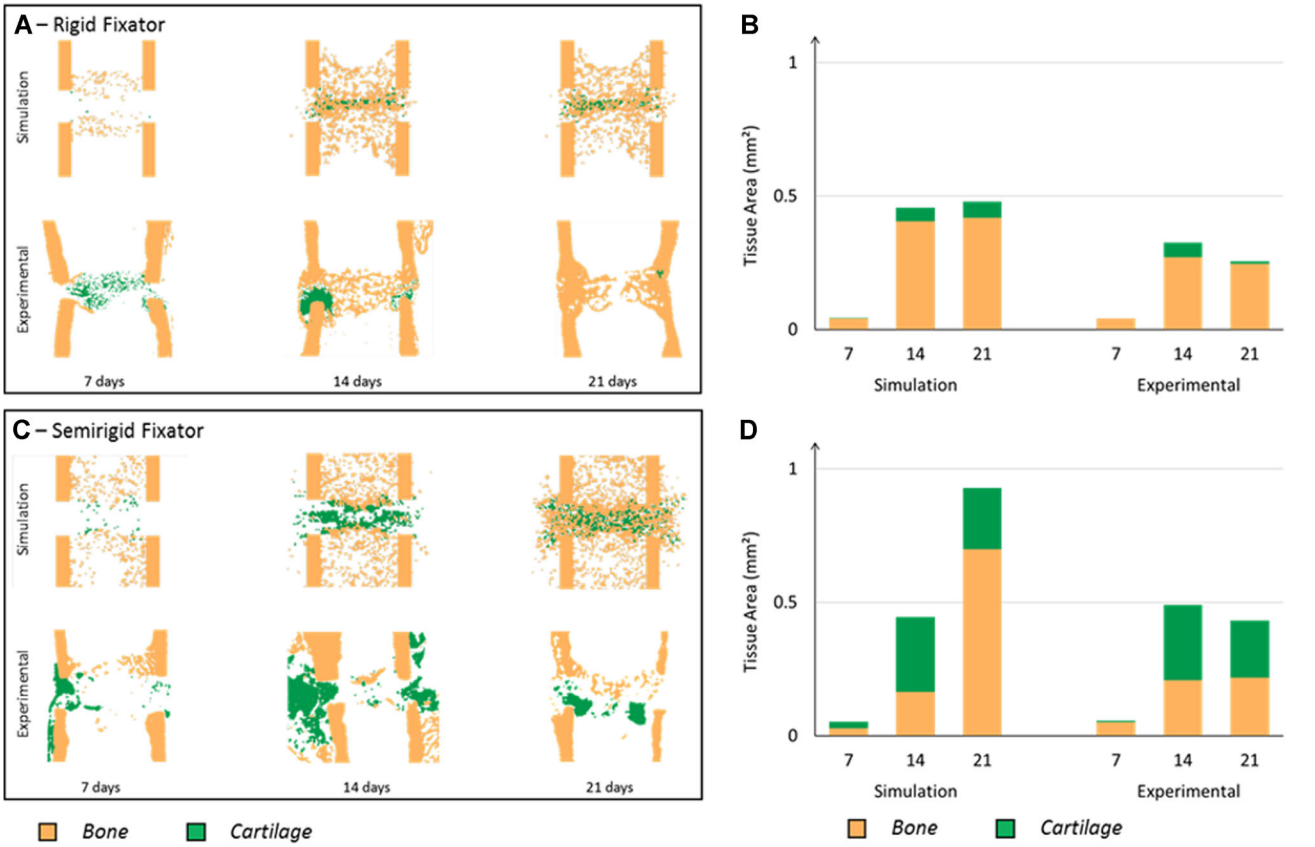

Fig. 5. In silico and in vivo tissue patterning in adult mice under rigid (*A*) or semirigid (*C*) external fixation. Bone and cartilage area measured in vivo and in silico under rigid (*B*) or semirigid (*D*) external fixation.

Table 5. Bone Tissue Area (mm^2) Predicted In Silico From Each Simulated Experiment at 7, 14, and 21 Days Under Rigid and Semirigid Mechanical Conditions

	Rigid fixator			Semirigid fixator		
Experiment	Day 7	Day 14	Day 21	Day 7	Day 14	Day 21
E1	0.01	0.07	0.04	0.01	0.15	0.18
E2	0.01	0.13	0.37	0.01	0.06	0.19
E3	0.11	0.36	0.30	0.02	0.14	0.50
E4	0.06	0.07	0.06	0.12	0.23	0.17
E5	0.01	0.12	0.13	0.01	0.06	0.39
E6	0.01	0.13	0.20	0.01	0.21	0.42
E7	0.01	0.06	0.07	0.01	0.10	0.32
E8	0.02	0.20	0.27	0.01	0.11	0.32
E9	0.01	0.10	0.35	0.01	0.06	0.24
E10	0.01	0.06	0.04	0.01	0.10	0.28
E11	0.01	0.10	0.10	0.01	0.16	0.30
E12	0.01	0.12	0.21	0.01	0.06	0.49
E13	0.20	0.16	0.14	0.37	0.37	0.30
E14	0.29	0.20	0.12	0.06	0.27	0.36
E15	0.08	0.24	0.15	0.01	0.10	0.45
E16	0.04	0.08	0.07	0.08	0.28	0.25

Table 6. Analysis of Variance ANOVA Performed to Quantify the Significance of Each Parameter on Bone Tissue Formation at 7, 14, and 21 Days Under Rigid and Semirigid Mechanical Conditions

	Rigid fixator						Semirigid fixator					
	Day 7		Day 14		Day 21		Day 7		Day 14		Day 21	
Parameter	SSP (mm^2)	%TSS	SSP (mm^2)	%TSS	SSP (mm^2)	%TSS	SSP (mm^2)	%TSS	SSP (mm^2)	%TSS	SSP (mm^2)	%TSS
P1	0.01	10	0.00	0	0.00	2	0.01	6	0.01	5	0.00	1
P2	0.01	12	0.00	2	0.01	3	0.01	7	**0.02**	**13**	0.02	9
P3	**0.03**	**32**	**0.01**	**12**	0.00	1	**0.02**	**18**	**0.04**	**26**	0.01	5
P4	0.00	3	0.00	5	0.00	1	0.00	2	0.00	0	0.01	6
P5	**0.02**	**18**	0.00	4	0.00	0	**0.01**	**11**	0.01	5	0.00	1
P6	**0.02**	**16**	0.01	6	0.00	0	0.01	10	0.02	**13**	**0.03**	**18**
P7	0.00	3	0.00	1	0.00	0	0.00	2	0.00	0	0.00	2
P8	0.00	0	0.00	3	0.00	0	0.00	1	0.00	2	0.00	1
P9	0.00	0	0.00	0	**0.03**	**15**	0.01	6	0.00	1	0.01	6
P10	0.00	1	0.00	5	0.00	3	0.01	6	0.01	4	0.00	0
P11	0.00	0	**0.01**	**14**	0.00	0	0.00	1	0.00	0	**0.03**	**20**
P12	0.00	2	0.01	8	0.00	0	**0.01**	**11**	0.00	2	0.01	8
P13	0.00	1	0.00	1	**0.04**	**23**	0.01	4	0.00	1	0.00	2
P14	0.00	0	0.00	3	0.00	2	0.01	4	0.00	0	0.00	0
P15	0.00	3	**0.03**	**36**	**0.09**	**49**	0.01	10	**0.04**	**27**	**0.03**	**19**

The sum of the squares (SSP) and the percentage of the total sum of squares (%TSS) was reported for each parameter.
The three most influential parameters at each time point for both mechanical conditions are in bold.

conditions. In fact, cartilage area extension peak was predicted between days 10 and 13 with values analogue to the experimental ones at day 14 (P15: day 11, 0.12 mm^2; P6 + P15: day 12, 0.12 mm^2; P11 + P15: day 11, 0.13 mm^2; P6 + P11 + P15: day 13, 0.14 mm^2) (Fig. 8).

Discussion

In this study, we identified the main contributors to age-related alterations in the mechanical regulation of bone healing using a combined in vivo/in silico approach. Experimentally, we determined that fixation stability effect leads to minor changes in bone healing in elderly mice compared with adult. Using a mouse femoral osteotomy model, we show that under rigid external fixation, both adult and elderly mice present similar healing progression. However, under semirigid conditions, adult mice showed a strong delay of the bone-healing response, while elderly mice showed only a small alteration in the progression of healing. This is surprising because it was previously thought that independent of age, there was a window of mechanical stability that led to enhanced bone healing. Studies investigating the effects of fixation stiffness on fracture healing have found that extremely rigid fixation can suppress bone formation,[38,39] whereas too flexible fixation can result in prolonged endochrondral ossification and hypertrophic nonunions.[40,41] Our study shows that unlike adult mice, strikingly, elderly mice were insensitive to increased mechanical instability. Computer models showed that the altered bone-healing response to changes in fixation stiffness with age could be explained by alterations in cellular mechanoresponse.

We did not observe a decrease in the healing capacity of elderly animals compared with adult animals under rigid fixation. We only observed a significantly reduced callus area and connective tissue area at day 7 in elderly mice. At 14 and 21 days, no effect of aging was found in any of the histomorphometric or micro-CT parameters analyzed. These results agree with Lu and colleagues, who found a similar bone-healing response in adult and elderly mice in non-stabilized tibia fractures.[42] The study was limited in the number of samples, particularly in elderly animal groups. Thus, we cannot rule out that the lack of age-related or fixation-related effect on tissue formation parameters (ie, bone tissue area, cartilage tissue area, etc.) observed was not due to a type II error related to our small sample size. However, healing scores clearly showed an effect of aging on the bone-healing response to changes in fixation stiffness. After 21 days, complete bridging was observed in most of the elderly animals under both fixation conditions. In contrast, in adult mice, while under rigid external fixation most animals showed complete bridging, under semirigid fixation most of the animals showed incomplete healing with little endosteal bone formation. Our results show that aging influences the effect of mechanical stability on fracture healing. While adult mice responded to decrease in fixation stability (from rigid to semirigid) with a prolonged endochondral ossification and a delay in healing, mild effects of fixation stability were found on the healing of elderly animals. This agrees with a previous study in rats, where we showed that fixation stability did not significantly impact bone healing in aged animals, while it influences healing in adult animals.[32] In contrast, Histing and colleagues showed delayed healing and remodeling in nonstabilized compared with stabilized fractures in aged mice,[33] which they explained as a consequence of the higher interfragmentary movement and a potential disruption of the vasculature. Interestingly, they did not observe any differences in protein expression within the callus due to changes in fixation stability. It might be that the differences in the induced strains within the callus between their stabilized and nonstabilized fractures were higher than those induced in this study by using a rigid and a semirigid fixator. For both age groups, our osteotomy fixation provided a twofold difference in the strains within the callus with higher strains in the

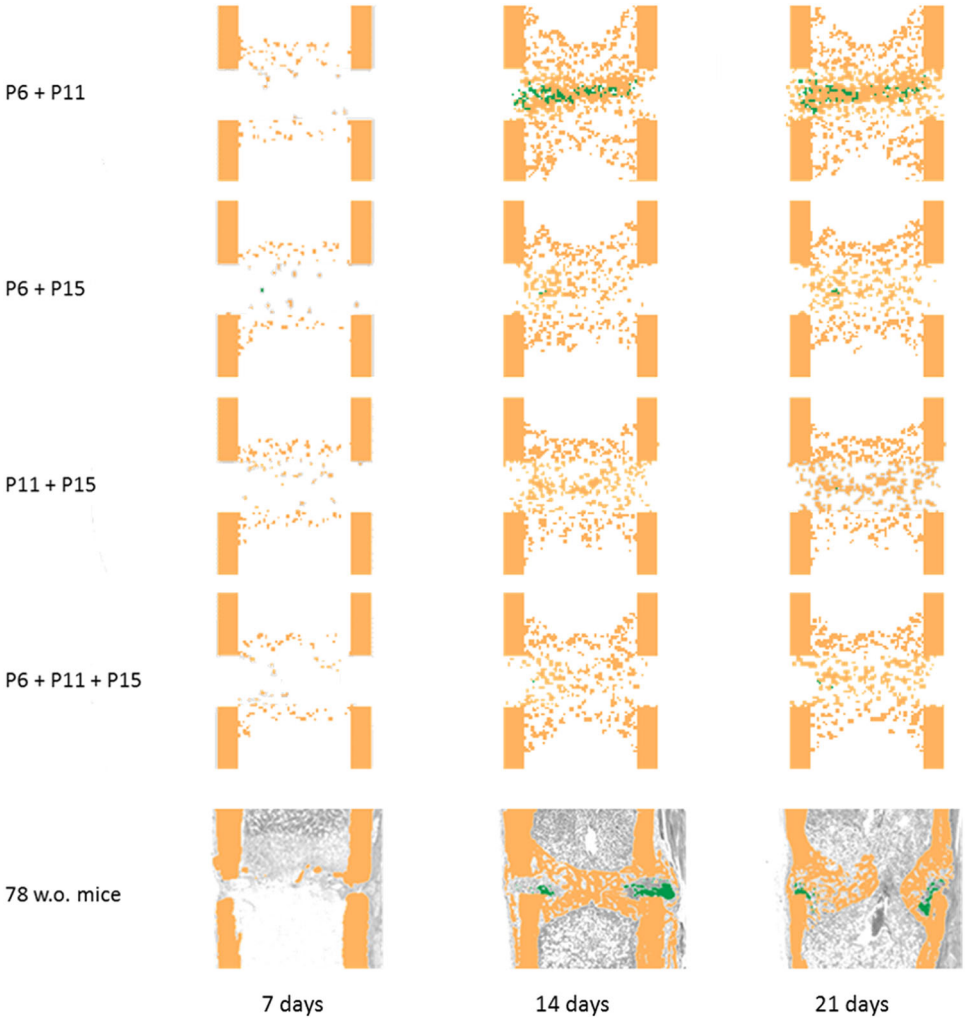

Fig. 6. (Top four rows) Tissue patterning in bone-healing simulations under rigid fixation and age-related alterations of the most influential parameters according to the design of experiments. (Bottom row) Tissue patterning under rigid fixation in 78-week-old mice. P6 = MSC proliferation rate; P11 = fibroblast apoptosis rate; P15 = cellular mechanosensation. Yellow = bone tissue; green = cartilage.

semirigid group. Unfortunately, they did not provide information about the mechanical environment within their fracture and, therefore, results cannot be easily compared. We quantified angiogenesis in a few samples at the different time points and could not see any differences between groups. Since in our study, the aged animals healed as well as the adult animals and there was only an alteration in their response to changes in fixation stability, this does not point toward angiogenesis. However, this needs to be further investigated.

Using our combined in vivo/in silico approach, we could identify the effect of potential age-related alterations at the cellular level on tissue formation patterns over the course of healing. Previous studies have suggested that reduced number of cells or their proliferation or migration potential with aging contributes to a reduced healing capacity.[43] In this project, a design of experiments approach was used to investigate the most influential cell activity parameters on bone-healing predictions under both rigid and semirigid fixator. We determined a small influence of an age-related reduction in the initial cell number and their migration rate on predicted tissue formation patterns. A weak influence of these biological factors was also reported by Isaksson and colleagues in an in silico bone-healing study.[12] Experimentally, bone healing was observed to be influenced by aging mostly under semirigid conditions. Therefore, the three most influencing parameters determined with design of experiments under semirigid fixation were investigated as possible factors to explain age-related alterations observed in mice. Reduced mechanosensitivity was identified to play the leading role to describe the aging influence on bone healing in mice. Previous studies already observed reduced osteocytes in elderlies due to loss of sex hormones,[44] which could explain the altered mechanosensation.

Bone healing in adult mice was more affected by changes in fixation stability. Larger callus was predicted when semirigid external fixator conditions were simulated. This resulted in higher amount of bone and cartilage tissues predicted in adult mice at 21 days post-operation. This agrees with the experimental observations in adult mice, where healing stabilized by semirigid fixator was characterized by significantly higher total callus area than rigid stabilization.

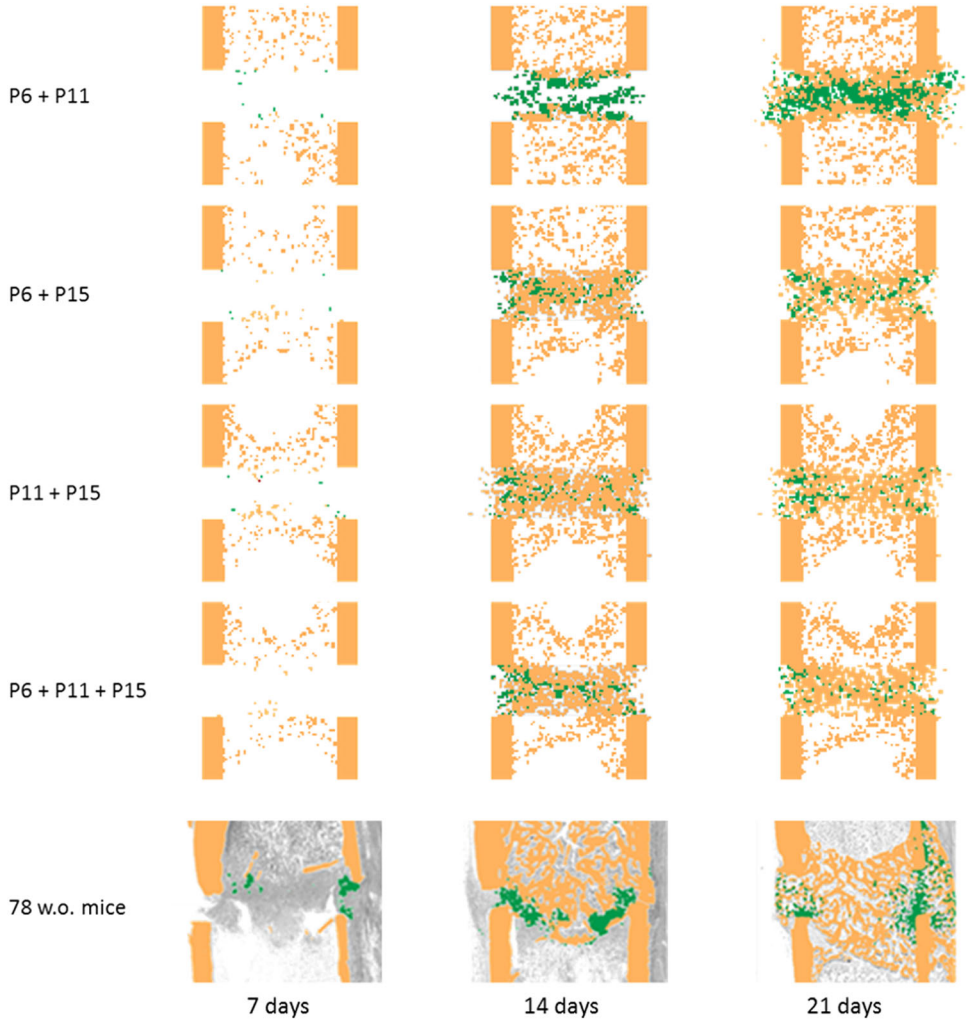

Fig. 7. (Top four rows) Tissue patterning in bone-healing simulations under semirigid fixation and age-related alterations of the most influential parameters according to the design of experiments. (Bottom row) Tissue patterning under semirigid fixation in 78-week-old mice. P6 = MSC proliferation rate; P11 = fibroblast apoptosis rate; P15 = cellular mechanosensation. Yellow = bone tissue; green = cartilage.

Age-related reduction of cellular mechanoresponse was simulated moving the differentiation ranges to higher mechanical stimuli. This resulted in wider zones of the ranges of mechanical stimuli beneficial for bone resorption or a null response. Under semirigid fixation, reduced mechanoresponse favorited the cellular differentiation into osteoblasts when compared with the baseline model. Higher mechanical stimuli were simulated under flexible conditions and led to favorite cartilage formation over bone in the adult mice. Reduced mechanosensitivity shifted the differentiation to osteoblasts to the detriment of chondrocyte differentiation. This resulted in larger bone area and minor amount of cartilage predicted due to reduced mechanosensitivity in the first days post-operation.

Only a few studies have investigated the influence of changes in cellular mechanoresponse on bone-healing predictions.[45,46] Checa and colleagues and Wehner and colleagues investigated interspecies differences in the mechanical regulation of healing, concluding that different specifies respond to different ranges of mechanical stimuli.[20,40] To our knowledge, this is the first study that investigates age-related alterations in cellular mechanoresponse during bone healing. Alterations in the bone response to mechanical loading with age have been extensively investigated in the context of bone adaptation.[39,41,47,48] It has been suggested that aging leads to a shift in the mechanical strain thresholds, leading to bone formation or resorption.[49] Here we adopted this concept and modified the ranges of mechanical stimuli leading to bone, cartilage, and fibrous tissue to simulate potential age-related effects. The proposed age-related reduction of mechanosensitivity was implemented as shift of differentiation thresholds to higher value. This correctly predicts the mechanoregulation in elderly mice, suggesting that higher mechanical stimuli are needed to induce a cell response. Although computer-model predictions led to good agreement with experimental data, other mechanisms might also play a role. Razi and colleagues showed a dysregulation in the bone-remodeling response to mechanical loading with age, although did not identify any

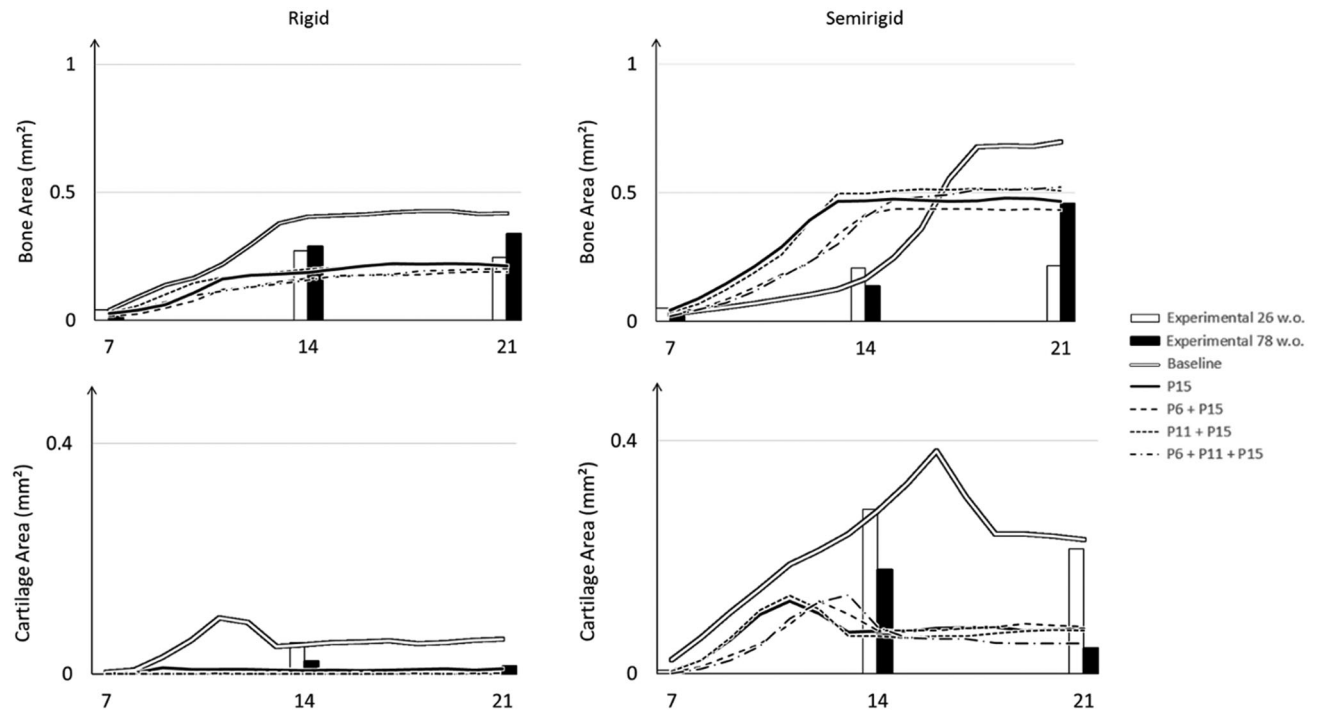

Fig. 8. Bone tissue and cartilage area (mm^2) under both rigid and semirigid external fixation. Experimental data from adult (white) and elderly (black) mice is reported in bars for 7, 14, and 21 days post-operation. In silico predictions at every time point are reported as curves: white lines = adults; black lines = age-related altered models.

changes in the mechanical thresholds required to initiate formation or resorption.[29] The influence of other parameters related to cellular mechanoresponse need to be further investigated in the future.

This study has several limitations. In adult mice, the model was not able to reproduce the decrease of cartilage tissue area between 14 and 21 days observed in vivo under rigid fixation. Our model reached a mechanical equilibrium after approximately 14 days, where no further changes in tissue phenotypes were predicted. This indicates that, in the model, the boundaries in the mechanical strains inducing bone and cartilage tissue formation are not sensitive enough to predict the endochondral ossification process. This is a limitation of the model that needs to be further investigated.

Under rigid conditions, reduced mechanosensitivity predicted decreased bone formation, which was not observed experimentally (Fig. 8). That could be a consequence of the extended silent and resorption zones due to reduced mechanosensitivity (Supplemental Table S1). Anyway, simulated reduced cellular mechanoresponse led to null response in cartilage formation with rigid fixator, as observed in elderly mice. Under the new mechanoregulatory rule, the higher strains necessary to differentiate MSC into chondrocytes were hardly reached within the fracture under rigid fixation. Future models should update our proposed mechanoregulation rule to simulate enhancement of bone tissue production but keep cartilage difficult to form under rigid conditions.

Under semirigid conditions, the investigated age-related reduced mechanoresponse correctly predicted the overall bone and cartilage tissue dynamics. However, both cartilage and bone tissue formation were predicted to happen slightly faster. It should be pointed out that age-related alterations in cellular activity parameters were not done to match any experimental data; instead, 20% or 50% alterations were tested to investigate potential mechanisms behind in vivo observations. It is to be expected that cellular activities might be altered at different levels and that the combination of those alterations result in the specific dynamic observed in vivo. In silico results predicted under semirigid conditions that combined reduced mechanoresponse, MSC proliferation rate, and fibroblast apoptosis rate leads to a slowdown in the healing process compared with only reduced mechanoresponse. Further studies are needed to understand the specific relative alterations in cellular activity.

The computer models of bone healing were not able to fully capture the bone-remodeling process at the later healing stages. Although our computer model includes the process of bone resorption in regions under low mechanical stimuli, the remodeling response is slower than the one observed experimentally. Several computer models have investigated bone remodeling during the bone-healing process using in silico approaches.[50–54] They have shown a strong influence of the external mechanical loads and the type and magnitude of mechanical stimuli used to drive the remodeling response. Future studies should further investigate how this healing phase is driven by mechanical signals.

Aging also leads to significant changes in the immune system.[55–57] Aging leads to an increased systemic pro-inflammatory status,[58,59] which has been associated with poorer fracture healing outcome[56,60,61]; however, the mechanisms remain poorly understood.[60] In this study, we did not directly investigate the role of inflammation on age-related

alterations in bone healing or how inflammation may affect the healing response to changes in mechanical stability. Future studies should aim to understand these interactions using both in vivo and in silico approaches.

In summary, the combined in vivo/in silico approach allowed us to document a decrease in the bone-healing response to changes in fixation stability with age. While adult mice showed a clear response to changes in fixation stability, this effect was absent in elderly mice. This reduced effect of mechanics in aged animals during healing can be explained by a reduced cellular mechanoresponse. This has clinical implications in the selection of the optimal fixation stability, which seems to be more sensitive in adult compared with elderly patients. Moreover, reduced cellular mechanoresponse in aging would imply a reduced response to physical therapy, which has been shown to improve the healing outcome.

Disclosures

The authors declare that there is no conflict of interest.

Acknowledgments

This study was funded by the German Research Foundation (Deutsche Forschungsgemeinschaft; WI 3761/4-1, DU298/14-1; CH 1123/4-1). We thank Mario Thiele for help with micro-CT analyses.

Authors' roles: GND, BMW and SC designed the study. BMW, CF and BK conducted the in vivo studies on mice. CF collected histological images, quantified histomorphometry and microCT data and performed statistical analysis. EB conducted in silico studies and performed design of experiments analysis. All the authors performed data interpretation. EB, CF and SC wrote the manuscript with contributions from all the authors.

References

1. Meyer RA, Tsahakis PJ, Martin DF, Banks DM, Harrow ME, Kiebzak GM. Age and ovariectomy impair both the normalization of mechanical properties and the accretion of mineral by the fracture callus in rats. J Orthop Res. 2001;19:428–35.
2. Skak SV, Jensen TT. Femoral-shaft fracture in 265 children—log-normal correlation with age of speed of healing. Acta Orthop Scand. 1988;59:704–7.
3. Gomberg BF, Gruen GS, Smith WR, Spott M. Outcomes in acute orthopaedic trauma: a review of 130,506 patients by age. Injury. 1999;30:431–7.
4. Nilsson BE, Edwards P. Age and fracture healing: a statistical analysis of 418 cases of tibial shaft fractures. Geriatrics. 1969;24:112–7.
5. Kasper G, Mao L, Geissler S, et al. Insights into mesenchymal stem cell aging: involvement of antioxidant defense and actin cytoskeleton. Stem Cells. 2009;27:1288–97.
6. Geissler S, Textor M, Kuhnisch J, et al. Functional comparison of chronological and in vitro aging: differential role of the cytoskeleton and mitochondria in mesenchymal stromal cells. PloS One. 2012;7:e52700.
7. Yukata K, Xie C, Li TF, et al. Aging periosteal progenitor cells have reduced regenerative responsiveness to bone injury and to the anabolic actions of PTH 1-34 treatment. Bone. 2014;62:79–89.
8. D'Ippolito G, Schiller PC, Ricordi C, Roos BA, Howard GA. Age-related osteogenic potential of mesenchymal stromal stem cells from human vertebral bone marrow. J Bone Miner Res. 1999;14:1115–22.
9. Lu CY, Hansen E, Sapozhnikova A, Hu D, Miclau T, Marcucio RS. Effect of age on vascularization during fracture repair. J Orthop Res. 2008;26:1384–9.
10. Checa S, Hesse B, Roschger P, et al. Skeletal maturation substantially affects elastic tissue properties in the endosteal and periosteal regions of loaded mice tibiae. Acta Biomater. 2015;21:154–64.
11. Aido M, Kerschnitzki M, Hoerth R, et al. Effect of in vivo loading on bone composition varies with animal age. Exp Gerontol. 2015;63:48–58.
12. Isaksson H, van Donkelaar CC, Huiskes R, Yao J, Ito K. Determining the most important cellular characteristics for fracture healing using design of experiments methods. J Theor Biol. 2008;255:26–39.
13. Schell H, Epari DR, Kassi JP, Bragulla H, Bail HJ, Duda GN. The course of bone healing is influenced by the initial shear fixation stability. J Orthop Res. 2005;23:1022–8.
14. Epari DR, Schell H, Bail HJ, Duda GN. Instability prolongs the chondral phase during bone healing in sheep. Bone. 2006;38:864–70.
15. Goodship AE, Cunningham JL, Kenwright J. Strain rate and timing of stimulation in mechanical modulation of fracture healing. Clin Orthop Relat R. 1998;355(Suppl):S105–15.
16. Claes LE, Heigele CA. Magnitudes of local stress and strain along bony surfaces predict the course and type of fracture healing. J Biomech. 1999;32:255–66.
17. Prendergast PJ, Huiskes R, Soballe K. Biophysical stimuli on cells during tissue differentiation at implant interfaces. J Biomech. 1997;30:539–48.
18. Carter DR, Blenman PR, Beaupre GS. Correlations between mechanical-stress history and tissue differentiation in initial fracture-healing. J Orthop Res. 1988;6:736–48.
19. Borgiani E, Duda GN, Willie B, Checa S. Bone healing in mice: does it follow generic mechano-regulation rules? Facta Universitatis Ser Mech Eng. 2015;13:217–27.
20. Checa S, Prendergast PJ, Duda GN. Inter-species investigation of the mechano-regulation of bone healing: comparison of secondary bone healing in sheep and rat. J Biomech. 2011;44:1237–45.
21. Vetter A, Witt F, Sander O, Duda GN, Weinkamer R. The spatio-temporal arrangement of different tissues during bone healing as a result of simple mechanobiological rules. Biomech Model Mechanobiol. 2012;11(1–2):147–60.
22. Andreykiv A, van Keulen F, Prendergast PJ. Simulation of fracture healing incorporating mechanoregulation of tissue differentiation and dispersal/proliferation of cells. Biomech Model Mechan. 2008;7:443–61.
23. Isaksson H, Wilson W, van Donkelaar CC, Huiskes R, Ito K. Comparison of biophysical stimuli for mechano-regulation of tissue differentiation during fracture healing. J Biomech. 2006;39:1507–16.
24. Garcia-Aznar JM, Kuiper JH, Gomez-Benito MJ, Doblare M, Richardson JB. Computational simulation of fracture healing: influence of interfragmentary movement on the callus growth. J Biomech. 2007;40:1467–76.
25. Gomez-Benito MJ, Garcia-Aznar JM, Kuiper JH, Doblare M. Influence of fracture gap size on the pattern of long bone healing: a computational study. J Theor Biol. 2005;235:105–19.
26. Hayward LNM, Morgan EF. Assessment of a mechano-regulation theory of skeletal tissue differentiation in an in vivo model of mechanically induced cartilage formation. Biomech Model Mechan. 2009;8:447–55.
27. Loboa EG, Beaupre GS, Carter DR. Mechanobiology of initial pseudarthrosis formation with oblique fractures. J Orthop Res. 2001;19:1067–72.
28. Lacroix D, Prendergast PJ. A mechano-regulation model for tissue differentiation during fracture healing: analysis of gap size and loading. J Biomech. 2002;35:1163–71.
29. Razi H, Birkhold AI, Weinkamer R, Duda GN, Willie BM, Checa S. Aging leads to a dysregulation in mechanically driven bone formation and resorption. J Bone Miner Res. 2015;30:1864–73.
30. Willie BM, Birkhold AI, Razi H, et al. Diminished response to in vivo mechanical loading in trabecular and not cortical bone in

adulthood of female C57Bl/6 mice coincides with a reduction in deformation to load. Bone. 2013;55:335–46.

31. Strube P, Sentuerk U, Riha T, et al. Influence of age and mechanical stability on bone defect healing: age reverses mechanical effects. Bone. 2008;42:758–64.
32. Mehta M, Strube P, Peters A, et al. Influences of age and mechanical stability on volume, microstructure, and mineralization of the fracture callus during bone healing: is osteoclast activity the key to age-related impaired healing? Bone. 2010;47:219–28.
33. Histing T, Heerschop K, Klein M, et al. Effect of stabilization on the healing process of femur fractures in aged mice. J Invest Surg. 2016;29:202–8.
34. Kruck B, Zimmermann EA, Figge C, et al. Sclerostin neutralizing antibody treatment enhances bone formation but does not rescue mechanically induced delayed healing. J Bone Miner Res. 2018;33(9):1686–97.
35. Hoerth RM, Kerschnitzki M, Aido M, et al. Correlations between nanostructure and micromechanical properties of healing bone. J Mech Behav Biomed Mater. 2018;77:258–66.
36. Wilson CJ, Schuetz MA, Epari DR. Effects of strain artefacts arising from a pre-defined callus domain in models of bone healing mechanobiology. Biomech Model Mechan. 2015;14:1129–41.
37. Taguchi G, Chowdhurry S, Wu Y. *Taguchi's quality engineering handbook*. Hoboken, NJ: John Wiley & Sons, Inc; 2005.
38. Brown ML, Yukata K, Farnsworth CW, et al. Delayed fracture healing and increased callus adiposity in a C57BL/6J murine model of obesity-associated type 2 diabetes mellitus. PloS One. 2014;9:e99656.
39. Birkhold AI, Razi H, Duda GN, Weinkamer R, Checa S, Willie BM. The influence of age on adaptive bone formation and bone resorption. Biomaterials. 2014;35:9290–301.
40. Wehner T, Steiner M, Ignatius A, Claes L. Prediction of the time course of callus stiffness as a function of mechanical parameters in experimental rat fracture healing studies—a numerical study. PloS One. 2014;9:e115695.
41. Silbermann M, Barshiramaymon B, Coleman R, et al. Long-term physical exercise retards trabecular bone loss in lumbar vertebrae of aging female mice. Calcif Tissue Int. 1990;46:80–93.
42. Lu C, Miclau T, Hu D, et al. Cellular basis for age-related changes in fracture repair. J Orthop Res. 2005;23:1300–7.
43. Yukata K, Xie C, Li TF, et al. Aging periosteal progenitor cells have reduced regenerative responsiveness to bone injury and to the anabolic actions of PTH 1-34 treatment. Bone. 2014;62:79–89.
44. Nordin BE, Need AG, Chatterton BE, Horowitz M, Morris HA. The relative contributions of age and years since menopause to postmenopausal bone loss. J Clin Endocrinol Metab. 1990;70(1):83–8.
45. Luu YK, Capilla E, Rosen CJ, et al. Mechanical stimulation of mesenchymal stem cell proliferation and differentiation promotes osteogenesis while preventing dietary-induced obesity. J Bone Miner Res. 2009;24:50–61.
46. Rubin CT, Capilla E, Luu YK, et al. Adipogenesis is inhibited by brief, daily exposure to high-frequency, extremely low-magnitude mechanical signals. Proc Natl Acad Sci U S A. 2007;104:17879–84.
47. Hoshi A, Watanabe H, Chiba M, Inaba Y. Effects of exercise at different ages on bone density and mechanical properties of femoral bone of aged mice. Tohoku J Exp Med. 1998;185:15–24.
48. Srinivasan S, Agans SC, King KA, Moy NY, Poliachik SL, Gross TS. Enabling bone formation in the aged skeleton via rest-inserted mechanical loading. Bone. 2003;33:946–55.
49. Turner CH, Takano Y, Owan I. Aging changes mechanical loading thresholds for bone-formation in rats. J Bone Miner Res. 1995;10:1544–9.
50. Repp F, Vetter A, Duda GN, Weinkamer R. The connection between cellular mechanoregulation and tissue patterns during bone healing. Med Biol Eng Comput. 2015;53:829–42.
51. Lacroix D, Prendergast PJ. Three-dimensional simulation of fracture repair in the human tibia. Comput Methods Biomech Biomed Eng. 2002;5:369–76.
52. Byrne DP, Lacroix D, Prendergast PJ. Simulation of fracture healing in the tibia: mechanoregulation of cell activity using a lattice modeling approach. J Orthop Res. 2011;29:1496–503.
53. Burke DP, Kelly DJ. Substrate stiffness and oxygen as regulators of stem cell differentiation during skeletal tissue regeneration: a mechanobiological model. PloS One. 2012;7:e40737.
54. Isaksson H, van Donkelaar CC, Huiskes R, Ito K. Corroboration of mechanoregulatory algorithms for tissue differentiation during fracture healing: comparison with in vivo results. J Orthop Res. 2006;24:898–907.
55. Montecino-Rodriguez E, Berent-Maoz B, Dorshkind K. Causes, consequences, and reversal of immune system aging. J Clin Invest. 2013;123(3):958–65.
56. Gibon E, Lu L, Goodman SB. Aging, inflammation, stem cells, and bone healing. Stem Cell Res Ther. 2016;7:44.
57. Weyand CM, Goronzy JJ. Aging of the immune system. Mechanisms and therapeutic targets. Ann Am Thorac Soc. 2016;13(Suppl):S422–8.
58. Michaud M, Balardy L, Moulis G, et al. Proinflammatory cytokines, aging, and age-related diseases. J Am Med Dir Assoc. 2013;14(12):877–82.
59. Franceschi C, Campisi J. Chronic inflammation (inflammaging) and its potential contribution to age-associated diseases. J Gerontol A Biol Sci Med Sci. 2014;69(Suppl):S4–9.
60. Clark D, Nakamura M, Miclau T, Marcucio R. Effects of aging on fracture healing. Curr Osteoporos Rep. 2017;15(6):601–8.
61. Toben D, Schroeder I, El Khassawna T, et al. Fracture healing is accelerated in the absence of the adaptive immune system. J Bone Miner Res. 2011;26(1):113–24.